Internal rotation and chlorine nuclear quadrupole coupling of o-chlorotoluene studied by microwave spectroscopy and ab initio calculations☆

D. Gerhard,[a] A. Hellweg,[a] I. Merke,[a,*] W. Stahl,[a] M. Baudelet,[b]
D. Petitprez,[b] and G. Wlodarczak[b]

[a] *Institut für Physikalische Chemie, RWTH Aachen, Templergraben 59, D-52062 Aachen, Germany*
[b] *Laboratoire PhLAM, CERLA, UMR CNRS 8523, Université de Lille 1, 59655 Villeneuve d'Ascq, France*

Abstract

The microwave spectrum of o-chlorotoluene has been reinvestigated using molecular beam Fourier transform microwave (MB-FTMW) spectrometers in the frequency range of 4–23 GHz. Due to the high resolution of this molecular beam technique the analysis yielded improved rotational constants, centrifugal distortion constants, and, for the first time, the complete chlorine nuclear quadrupole coupling tensor. From the torsional fine structure the barrier to internal rotation of the methyl group was found to be $5.5798(52)\,\text{kJ}\,\text{mol}^{-1}$. Experimental results and ab initio calculations are compared.
© 2003 Elsevier Science (USA). All rights reserved.

1. Introduction

Toluene and substituted toluenes, especially fluoro-toluenes, have been investigated by microwave spectroscopy [1–6] since decades, but only little effort has been spent on chlorotoluenes. Herberich [7] studied the microwave spectrum of p-chlorotoluene in 1967. The NMR spectrum of o-chlorotoluene in a liquid crystal was analyzed by Diehl et al. [8] in 1971. In their work the barrier to internal rotation of the methyl group was found to be $V_3 = 5.0(2.5)\,\text{kJ}\,\text{mol}^{-1}$ and a molecular structure was determined, where the methyl group is staggered with respect to the chlorine atom. The microwave spectrum of o-chlorotoluene was studied for the first time by Nair and Epple [9] in 1990 with a Stark spectrometer. The rotational constants as well as the diagonal elements of the chlorine quadrupole coupling tensors were determined for both chlorine isotopomers. No splittings due to internal rotation of the methyl group were observed, therefore, the authors concluded, that the V_3 barrier might be much higher than that one reported by Diehl et al. In 1999 Nair [10] reported on the assignment of the first excited torsional state on which also no splittings due to internal motion were detected with Stark spectroscopy. Using the intensity ratio of the ground and first excited state transitions, he calculated the potential barrier to $6.74(40)\,\text{kJ}\,\text{mol}^{-1}$. This value is in reasonable agreement with ab initio studies ($V_3 = 5.76(3)\,\text{kJ}\,\text{mol}^{-1}$) performed by Schaefer et al. [11] in 1992 and those of Richard et al. [12] in 1996 ($V_3 = 5.75\,\text{kJ}\,\text{mol}^{-1}$).

The objectives of this work are to improve the rotational constants and to determine centrifugal distortion constants and the complete quadrupole coupling tensor for both chlorine isotopomers. We were especially interested to obtain the barrier to internal rotation of the methyl group for the first time directly from the $A–E$ splittings in the rotorsional ground state spectrum and to compare the experimental results to related molecules and ab initio calculations.

2. Experimental

The experiments were performed with MB-FTMW spectrometers operating in the frequency range from 4 to 26.5 GHz [13,14]. Usually 4096 (4 K) or 8192 (8 K) data points were sampled at intervals of 40 ns. Depending on the linestrength 50–4000 fids were co-added. The sample was purchased from Lancaster, Mühlheim am Main, and used without further purifications. In the experiments performed with the spectrometer in Aachen the substance was kept in a small reservoir upstream the nozzle and helium was used as carrier gas at a stagnation pressure of 120 kPa. In Lille a mixture of about 1% substance in neon as carrier gas was used at a stagnation pressure of about 200 kPa. An example spectrum is shown in Fig. 1.

3. Spectral analysis

The rotational constants and chlorine nuclear quadrupole coupling constants of o-chlorotoluene were fairly well known from previous work [9] and we used them to predict the spectra of the ^{35}Cl and ^{37}Cl isotopomers. Almost all observed hyperfine components were found to be additionally split due to internal rotation. Assuming a reasonable torsional barrier we used the computer program XIAM [15] to assign the A and E state lines and to predict the width of the torsional (A–E) splittings. Unfortunately, XIAM treats nuclear quadrupole coupling only in an approximate way where the off-diagonal elements in J are neglected. Therefore, we decided to fit the A and E state lines separately using Pickett's program [16]. The effective Hamiltonian

$$\hat{H}_\Gamma = \hat{H}_{\mathrm{rot},\Gamma} + \hat{H}_{\mathrm{cd},\Gamma} + \hat{H}_{\mathrm{lin}P,\Gamma} + \hat{H}_{\mathrm{NQ},\Gamma}, \ \Gamma \in \{A, E\} \tag{1}$$

contains contributions from overall rotation $\hat{H}_{\mathrm{rot},\Gamma}$, centrifugal distortion $\hat{H}_{\mathrm{cd},\Gamma}$, and nuclear quadrupole coupling $\hat{H}_{\mathrm{NQ},\Gamma}$. The term $\hat{H}_{\mathrm{lin}P,\Gamma}$ is linear in the components $\hat{P}_g$, $g \in \{a, b, c\}$ of the angular momentum operator $\hat{P}$.

In detail, we used the rigid rotor Hamiltonian

$$\hat{H}_{\mathrm{rot},\Gamma} = A_\Gamma \hat{P}_a^2 + B_\Gamma \hat{P}_b^2 + C_\Gamma \hat{P}_c^2 \tag{2}$$

to describe the overall rotation. It should be noted that the effective rotational constants are contaminated by internal rotation.

The centrifugal distortion is treated using Watson's A reduction [17] in the I^r representation.

$$
\begin{aligned}
\hat{H}_{\mathrm{cd},\Gamma} = & -\Delta_{J,\Gamma}\hat{P}^4 - \Delta_{JK,\Gamma}\hat{P}^2\hat{P}_a^2 - \Delta_{K,\Gamma}\hat{P}_a^4 \\
& - 2\delta_{J,\Gamma}\hat{P}^2(\hat{P}_b^2 - \hat{P}_c^2) - \delta_{K,\Gamma}[\hat{P}_a^2(\hat{P}_b^2 - \hat{P}_c^2) \\
& - (\hat{P}_b^2 - \hat{P}_c^2)\hat{P}_a^2].
\end{aligned} \tag{3}
$$

Also in this case small amounts of internal rotation is included in the centrifugal distortion parameters.

The coupling between internal and overall rotation is described by

$$\hat{H}_{\mathrm{lin}P,\Gamma} = D_{a,\Gamma}\hat{P}_a + D_{b,\Gamma}\hat{P}_b + D_{c,\Gamma}\hat{P}_c. \tag{4}$$

It is only needed for fitting the E state lines. For the A state the parameters $D_{g,A}$ are zero and the whole operator vanishes, i.e., $\hat{H}_{\mathrm{lin}P,A} = 0$.

Finally, nuclear quadrupole coupling is treated in the usual way as the product of the second rank spherical tensor operators of the electric field gradient V and the nuclear quadrupole moment Q. It is

$$\hat{H}_{\mathrm{NQ},\Gamma} = \hat{V}_\Gamma^{(2)} \cdot \hat{Q}^{(2)} \tag{5}$$

A complete list of all measured transitions of o-chlorotoluene of both, the ^{35}Cl and the ^{37}Cl isotopomer is available as supplementary material (Table S1 and S2, respectively). A few selected transitions are given in Table 1. The molecular parameters resulting from the least squares fits are compiled in Table 2. From these parameters all transitions could be calculated within the experimental error limits.

4. Ab initio calculations

To compare our experimental results with first principle methods we used the Gaussian 98 [18] ab initio package. The shape of the torsional potential $V(\alpha)$ of the methyl group was determined by varying the dihedral angle of one methyl hydrogen from 0° to 120° relative to the molecular frame in steps of 15° on MP2/6-311G** level. We only fixed this dihedral angle allowing all other parameters to relax. For the numbering of atoms see Fig. 2. The initial C_{3v} symmetry of the methyl group was slightly distorted showing dihedral angles ∠(H7,C2,C7, H8) and ∠(H8,C2,C7,H9) between 118.4° and 121.6°.
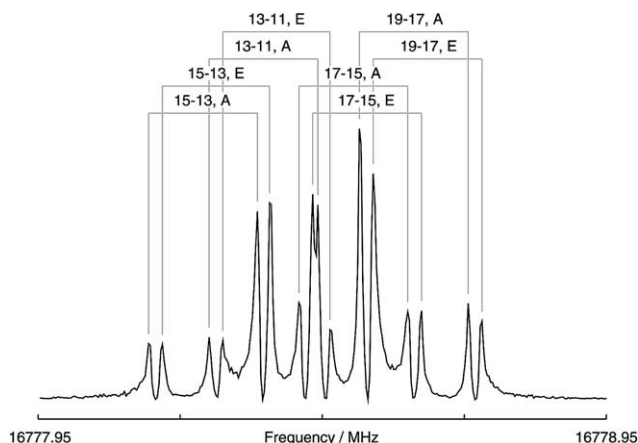

Fig. 1. The 8_{18}–7_{17} transition of [^{37}Cl]-o-chlorotoluene. All ^{37}Cl quadrupole hyperfine components (designated by $2F$ values) are split into A and E torsional components, which are additionally split due to the Doppler effect.

Table 1
Selected[a] microwave frequencies of *o*-chlorotoluene

J'	K_a'	K_c'	$2F'$	J	K_a	K_c	$2F$	v_A[b]	δ_A[c]	v_E[b]	δ_E[c]
[^{35}Cl]-*o*-chlorotoluene											
2	1	2	7	1	0	1	5	5866.3501	4.6	5866.3228	5.5
			5				3	5875.4763	0.2	5875.4494	0.5
			3				1	5850.5426	0.9	5850.5140	−0.3
3	0	3	9	2	0	2	7	7149.0971	0.5	7149.0660	0.2
			7				5	7150.0484	−0.4	7150.0175	−0.4
			5				3	7145.5917	−0.9	7145.5609	−0.3
			3				1	7144.7154	0.2	7144.6843	0.1
			7				7	7133.9407	−1.1	7133.9092	−1.2
			5				5	7157.1539	−0.5	7157.1228	−1.2
			3				3	7160.7857	0.2	7160.7539	−1.3
			5				7	7141.0451	−2.4	7141.0137	−2.8
			3				5	7172.3455	−1.8	7172.3159	−2.0
6	4	3	15	5	4	2	13	15686.2750	1.0	15687.5730	0.0
			13				11	15678.2780	0.8	15679.5860	2.8
			11				9	15680.6380	−0.6	15681.9360	−4.6
			9				7	15688.5730	−0.5	15689.8750	2.0
7	0	7	17	6	1	6	15	15041.3270	0.5	15041.2976	−4.3
			15				13	15041.0780	0.2	15041.0535	0.4
			13				11	15040.6570	−0.3	15040.6327	0.1
			11				9	15040.9083	0.4	15040.8836	0.3
[^{37}Cl]-*o*-chlorotoluene											
3	0	3	9	2	0	2	7	7020.1360	0.2	7020.1069	1.9
			7				5	7020.8631	−2.5	7020.8354	0.4
			5				3	7017.3361	−0.9	7017.3062	0.5
			3				1	7016.6606	−1.7	7016.6312	0.0
6	4	3	15	5	4	2	13	15319.3300	0.1	15320.8020	−1.5
			13				11	15313.0200	0.0	15314.4970	0.1
			11				9	15314.8570	−1.0	15316.3360	1.7
			9				7	15321.1790	−0.8	15322.6520	−0.1
8	1	8	19	7	1	7	17	16778.6339	1.7	16778.6110	1.1
			17				15	16778.5265	−0.5	16778.5042	−0.5
			15				13	16778.2603	−1.4	16778.2380	−1.4
			13				11	16778.3673	0.5	16778.3441	−0.3

[a] A complete list of observed microwave frequencies is available as supplementary material (Tab. S1 and S2).

[b] v_A, v_E, transition frequencies of the *A* and *E* species in MHz.

[c] δ_A, δ_E, observed − calculated values in kHz.

Therefore, we defined a medium rotational angle α of the methyl group according to [19]: $\alpha = (\angle(C1, C2, C7, H7) + \angle(C1, C2, C7, H8) + \angle(C1, C2, C7, H9) − 360°)/3$. In Fig. 2 $\angle(C1,C2,C7,H7)$ has been drawn as 180°. This is the configuration of the lowest ab initio energy $E(\alpha)$ (equilibrium structure) to which all potential values $V(\alpha) = E(\alpha) − E(180°)$ were referred to. They are shown as small circles in Fig. 3. The V_3 and V_6 parameters of the potential function

$$V(\alpha) = \frac{V_3}{2}(1 + \cos 3\alpha) + \frac{V_6}{2}(1 + \cos 6\alpha) \qquad (6)$$

were fitted. The potential function calculated from V_3 and V_6 is also shown in Fig. 3. The calculated and experimental potential parameters are compared in Table 3.

The equilibrium structure was optimized by calculations at different basis sets and methods (HF, MP2, and B3LYP) where all structure parameters were allowed to relax. Looking at the ab initio calculations we found

that the structure is neither varying very much with the method nor with the basis set. In the basis sets 6-311G** and larger the maximum deviations were 2.0 pm for C–C bonds, 1.5 pm for C–H bonds, and 2.9 pm for the C–Cl bond. The maximum deviation of the bond angles was found to be 0.8°. All atom except two hydrogens of the methyl group were calculated to be in plane, i.e., the elevation angles above the ring plane were smaller than 0.004°. The maximum deviation of the dihedral angles describing the methyl hydrogens (see Table 4) is smaller than 0.4°. Our best structure, calculated on MP2/6-311+G(3df,2p) level, is given in Table 4.

The rotational constants, the angle $\angle(i, a)$, as well as the chlorine nuclear quadrupole coupling constants in the bond axis system resulting from this calculation are compared with experimental results in Table 3.

The moment of inertia of the methyl group I_α was obtained assuming the C2–C7 bond as a fixed axis of rotation. This does probably not reflect the real situa-

Table 2
Molecular constants of *o*-chlorotoluene

	[^{35}Cl]-*o*-chlorotoluene		[^{37}Cl]-*o*-chlorotoluene	
	A species	*E* species	*A* species	*E* species
A (MHz)	2851.366764(173)	2851.338343(289)	2842.57444(69)	2842.54691(92)
B (MHz)	1538.326455(95)	1538.305675(97)	1500.301532(299)	1500.280939(306)
C (MHz)	1005.373806(51)	1005.374270(54)	987.928321(107)	987.928818(109)
Δ_J (kHz)	0.04718(109)	0.04594(112)	0.0541(54)	0.0361(59)
Δ_{JK} (kHz)	0.1676(48)	0.1700(51)	0.1335(251)	0.231(35)
Δ_K (kHz)	0.2989(92)	0.2696(282)	0.538(146)	0.295(191)
δ_J (kHz)	0.01520(53)	0.01414(54)	0.01837(261)	0.00950(286)
δ_K (kHz)	0.1344(67)	0.1268(71)	0.1797(263)	0.1171(264)
D_a (MHz)	0.0	−1.77383(35)	0.0	−1.72795(159)
D_b (MHz)	0.0	−1.385(119)	0.0	−1.294(282)
χ_{aa} (MHz)	−67.97044(173)	−67.97356(174)	−53.88672(216)	−53.89052(216)
χ_{bb} (MHz)	36.41199(188)	36.41325(189)	29.01249(241)	29.01597(241)
χ_{ab} (MHz)	14.52(53)	15.47(51)	9.36(70)	10.93(61)
N	64	62	34	34
N_{hfs}	267	257	148	148
σ (kHz)	1.2	1.9	1.5	0.9

Note. Watson's *A* reduction and I^r representation used.

For D_a and D_b see Eq. (4).

N, number of different rotational transitions.

N_{hfs}, number of hyperfine components; σ, standard deviation of the fit.

tion, however, the result $I_\alpha = 3.128 \times 10^4$ u pm^2 is reasonable and we decided to keep it fixed at this value for all calculations throughout this paper.

The nuclear quadrupole coupling constants $\chi_{ii} = eq_{ii}Q$ were calculated using the chlorine electric field gradient tensor elements q_{ii}, $ii \in \{xx, yy, zz\}$, of the ab initio calculation and the nuclear quadrupole moment of chlorine $Q(^{35}\text{Cl}) = -81.65$ mbarn [20,21]. To obtain the respective coupling constants of the ^{37}Cl species, the ^{35}Cl values were divided by the ratio of the nuclear quadrupole moments $Q(^{35}\text{Cl})/Q(^{37}\text{Cl}) = 1.26889(3)$ [21,22]. The calculated coupling constants are compared with the experimental values in Table 3.
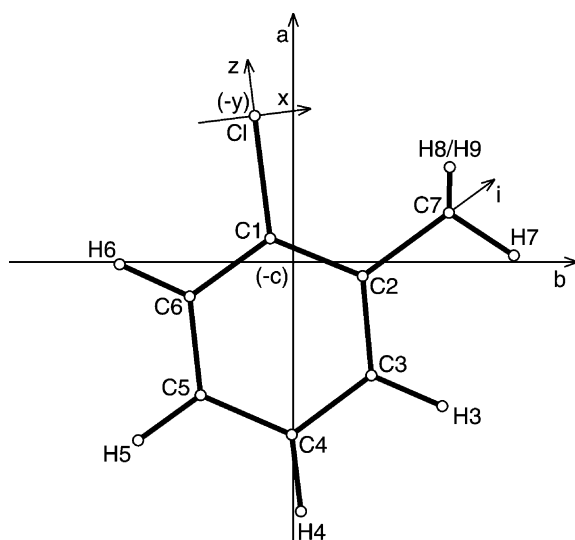
Many studies have shown that the principal z axis of the chlorine nuclear quadrupole coupling tensor coincides with the C–Cl bond axis. We therefore also calculated the angle $\angle(z,a)$ from our ab initio geometry, which is also compared with the respective experimental values in Table 3.

The reduced barrier height s is defined [23] as

$$s = \frac{4V_3}{9F}, \quad F = \frac{\hbar^2}{2I_\alpha r} \tag{7}$$

with the reduced rotational constant F of the methyl group. The latter quantity contains the already mentioned moment of inertia of the methyl group I_α and the reducing factor r given by

$$r = 1 - \sum_g \frac{\lambda_g^2 I_\alpha}{I_g}, \quad g = a, b, c. \tag{8}$$
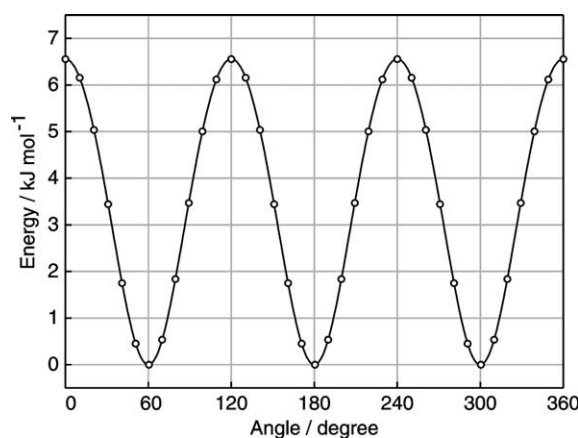

Fig. 2. Molecular geometry of *o*-chlorotoluene.

Fig. 3. Potential function of the methyl torsion of *o*-chlorotoluene as obtained from ab initio calculations.

Table 3
Derived molecular parameters and ab initio results of *o*-chlorotoluene

	[^{35}Cl]-*o*-chlorotoluene			[^{37}Cl]-*o*-chlorotoluene		
	Experimental	Ab initio	δ	Experimental	Ab initio	δ
A (MHz)	2851.347817(201)	2876.31	0.9	2842.55609(66)	2867.36	0.9
B (MHz)	1538.312602(72)	1541.65	0.2	1500.287803(227)	1503.56	0.2
C (MHz)	1005.374115(40)	1009.88	0.4	987.928652(81)	992.33	0.4
$\angle(i,a)$ (°)	57.75(18)	53.64	−7.1	58.61(60)	54.43	−7.1
$\angle(i,b)$ (°)	32.25(18)	36.36	12.7	31.39(60)	35.57	13.3
$\angle(i,c)$ (°)	90.0 (fixed)	90.00	–	90.0 (fixed)	90.00	–
I_α (10^4 u pm^2)	3.128 (fixed)	3.128	–	3.128 (fixed)	3.128	–
s	38.011(35)	44.36	16.7	38.00(12)	44.38	16.8
V_3 (THz)	13.983(13)	16.33	16.8	13.976(46)	16.33	16.8
V_3 (cm^{-1})	466.44(43)	544.7	16.8	466.2(15)	544.7	16.8
V_3 (kJ mol^{-1})	5.5798(52)	6.517	16.8	5.577(18)	6.517	16.8
V_6 (THz)	n.d.	−0.80	–	n.d.	−0.80	–
V_6 (cm^{-1})	n.d.	−26.7	–	n.d.	−26.7	–
V_6 (kJ mol^{-1})	n.d.	−0.32	–	n.d.	−0.32	–
χ_{xx} (MHz)	38.394(144)	37.37	−2.7	30.058(157)	29.45	−2.0
χ_{yy} (MHz)	31.55845(169)	30.92	−2.0	24.87423(222)	24.37	−2.0
χ_{zz} (MHz)	−69.953(144)	−68.30	−2.4	−54.933(157)	−53.82	−2.0
η	0.0977	0.0944	−3.4	0.0944	0.0944	0.0
$\angle(z,a)$ (°)	7.77(27)	7.27	−6.9	6.37(46)	6.48	1.7

Note. $\delta = [(\text{calc.} - \text{exp.})/\text{exp.}] \times 100$.
n.d. not determined.

Table 4
Bond distances, angles, and dihedral angles of *o*-chlorotoluene calculated on MP2/6-311+G(2df,2p) level

Distances (pm)		Angles (°)		Dihedral angles (°)[a]	
C1–C2	139.81	C1–C2–C3	116.97		
C2–C3	139.71	C2–C3–C4	121.83		
C3–C4	139.18	C3–C4–C5	119.75		
C4–C5	139.19	C4–C5–C6	119.85		
C5–C6	139.12				
C2–C7	149.74	C7–C2–C3	121.40		
C1–Cl	173.73	C6–C1–Cl	118.48		
C3–H3	108.27	C2–C3–H3	118.43		
C4–H4	108.10	C3–C4–H4	119.95		
C5–H5	108.11	C4–C5–H5	120.52		
C6–H6	108.06	C5–C6–H6	121.10		
C7–H7	108.71	C2–C7–H7	110.49	C1–C2–C7–H7	180.00
C7–H8	108.92	C2–C7–H8	111.05	C1–C2–C7–H8	59.42
C7–H9	108.92	C2–C7–H9	111.05	C1–C2–C7–H9	−59.42

[a] All atoms except H8 and H9 are in plane.

The calculation of the principal moments of inertia I_g of the (rigid) *o*-chlorotoluene molecule from atomic masses and ab initio structural parameters has been mentioned already. The direction cosines $\lambda_g = \cos \angle(i,g)$ have been calculated also from the ab initio structural data. Also the reduced barrier height s is compared with experimental values in Table 3.

5. Conclusion

In this section we will interpret the molecular constants obtained from the spectral analysis in terms of quantities directly related to the structural, dynamical,

and electronical properties of the molecule. Moreover we will compare them with our results obtained from ab initio calculations. Three aspects will be considered in detail: the molecular structure, the internal rotation of the methyl group, and the chlorine nuclear quadrupole coupling.

5.1. Molecular structure

Since we only investigated two different isotopomers (^{35}Cl and ^{37}Cl) the structural information directly available from the experimental data is rather limited. Nevertheless, these data can be compared with ab initio calculations (see Table 3).

All experimental rotational constants and their ab initio values were found to agree within 1%. A much better agreement cannot be expected since the ab initio calculations refer to the equilibrium structure whereas the experimental results reflect the vibrational ground state. The r_s coordinates [24] of ^{35}Cl are $|a_{Cl}| = 205.43(8)$ pm and $|b_{Cl}| = 53.9(3)$ pm. They are also in good agreement with the ab initio values $a_{Cl} = 205.16$ pm and $b_{Cl} = -54.24$ pm. The experimental errors of the r_s coordinates are calculated according to van Eijck [25].

The internal rotor axis i is obtained from the analysis of the methyl internal rotation given below. If we assume i to coincide with the C2–C7 bond axis i', we can compare the angles $\angle(i, a)$ and $\angle(i, b)$ with the ab initio values $\angle(i', a)$ and $\angle(i', b)$. We found a maximum deviation of $4.2°$ between these angles, which is slightly higher than expected. This may be due to the fact that the methyl group is distorted when it rotates.

The principal z axis of the Cl nuclear quadrupole coupling tensor is often assumed to coincide with the C–Cl bond axis z'. We found the angle $\angle(z, a)$ obtained from the analysis of the nuclear quadrupole coupling to agree within $0.5°$ with the angle $\angle(z', a)$ calculated by ab initio methods.

5.2. Methyl internal rotation

Now we will analyze the effective rotational constants A_Γ, B_Γ, C_Γ, $\Gamma \in \{A, E\}$, and the parameters D_g, $g \in \{a, b, c\}$, to obtain the (effective) barrier to internal rotation V_3 and the angles $\angle(i, g)$ between the internal rotor axis i and the principal axes of inertia (compare Fig. 1). For this purpose we use the equations resulting from a perturbation theoretical approach of the internal rotation problem [23]:

$$\Delta A = A_A - A_E = F\rho_a^2[W_A^{(2)} - W_E^{(2)}], \tag{9}$$

$$\Delta B = B_A - B_E = F\rho_b^2[W_A^{(2)} - W_E^{(2)}], \tag{10}$$

$$\Delta C = C_A - C_E = F\rho_c^2[W_A^{(2)} - W_E^{(2)}], \tag{11}$$

and

$$D_a = F\rho_a W_E^{(1)}, \tag{12}$$

$$D_b = F\rho_b W_E^{(1)}, \tag{13}$$

$$D_c = F\rho_c W_E^{(1)}. \tag{14}$$

F has been already introduced in Eq. (7). ρ_g is given by

$$\rho_g = \frac{\lambda_g I_\alpha}{I_g}. \tag{15}$$

The first and second order perturbation sums $W_E^{(1)} = W_{0,1}^{(1)}$ and $W_A^{(2)} = W_{0,0}^{(2)}$, $W_E^{(2)} = W_{0,1}^{(2)}$, respectively, are defined as [23]

$$W_{v,\sigma}^{(1)} = -2\langle v, \sigma|p|v, \sigma\rangle \tag{16}$$

$$W_{v,\sigma}^{(2)} = 1 + 4F\sum_{v'}' \frac{|\langle v, \sigma|p|v', \sigma\rangle|^2}{E_{v,\sigma} - E_{v',\sigma}}, \tag{17}$$

where $\langle v, \sigma|p|v', \sigma\rangle$ are the matrix elements of the internal angular momentum p in the basis of the hindered rotor wavefunctions $\psi_{v,\sigma}$. $E_{v\sigma}$ are the eigenvalues of the hindered rotor. The perturbation sums only depend on the reduced barrier height s.

The structural rotational constants A, B, and C are approximately obtained from the effective rotational constants by

$$A = \frac{1}{3}(A_A + 2A_E), \quad B = \frac{1}{3}(B_A + 2B_E),$$

$$C = \frac{1}{3}(C_A + 2C_E). \tag{18}$$

In the case of *o*-chlorotoluene $\angle(i, c) = 90°$ and therefore, $\lambda_c = 0$ and $\rho_c = 0$. Consequently, $\Delta C = C_A - C_E = 0$ and $D_c = 0$. Indeed, for the ^{35}Cl isotopomer ΔC was found to be $0.461(74)$ kHz, which is very small compared to $\Delta A = 28.44(34)$ kHz and $\Delta B = 20.77(14)$ kHz. However, the experimental value of ΔC is not zero within error limits what is probably due to vibrational contributions which are not included in our model. No attempts were made to fit the D_c constant. The angles $\angle(i, a)$ and $\angle(i, b)$ are connected by the equation $\lambda_a^2 + \lambda_b^2 = 1$. Generally, there are two independent possibilities to determine these angles.

(i) From Eqs. (9) and (10) we obtain

$$\angle(i, a) = \arccos\sqrt{\frac{B^2\Delta A}{A^2\Delta B + B^2\Delta A}},$$

$$\angle(i, b) = \arccos\sqrt{\frac{A^2\Delta B}{A^2\Delta B + B^2\Delta A}}. \tag{19}$$

(ii) Independently, Eqs. (12) and (13) can be used to derive

$$\angle(i, a) = \arccos\sqrt{\frac{B^2 D_a^2}{A^2 D_b^2 + B^2 D_a^2}},$$

$$\angle(i, b) = \arccos\sqrt{\frac{A^2 D_b^2}{A^2 D_b^2 + B^2 D_a^2}}. \tag{20}$$

Since the error of D_b is rather large, the angles given in Table 3 were calculated using Eq. (19). In a next step the reduced barrier to internal rotation s, which is the only parameter W_E^1 depends on, was fitted in Eq. (12). The result of the ^{35}Cl and the ^{37}Cl isotopic species $s = 38.011(35)$ and $s = 38.00(12)$, respectively, perfectly agree. However, the ab initio results were found to be by 16.8% larger than the experimental data. This deviation is large, but not unusual for such calculations. It should be kept in mind, that no corrections for zero point vibrations were made which are known to have a significant influence on the result.

Table 5
Torsional barriers of toluene derivatives

		V_3 (kJ mol^{-1})	Ref.
o-Tolunitrile	*o*-(CH$_3$,CN)–C$_6$H$_4$	2.245379(36)[a]	[27]
o-Fluorotoluene	*o*-(CH$_3$,F)–C$_6$H$_4$	2.717[a]	[3]
2,4-Difluorotoluene	*o*-(CH$_3$,F,F)–C$_6$H$_3$	2.4393(28)[a]	[28]
anti-o-Cresol	*anti-o*-(CH$_3$,OH)–C$_6$H$_4$	4.4256(14)	[29]
o-Chlorotoluene	*o*-(CH$_3$,Cl)–C$_6$H$_4$	5.527(10)	This work
o-Xylene	*o*-(CH$_3$,CH$_3$)–C$_6$H$_4$	6.201(38)[a]	[6]
syn-o-Cresol	*syn-o*-(CH$_3$,OH)–C$_6$H$_4$	7.912(46)	[29]

[a] Converted from other units to kJ mol^{-1}.

With Eq. (7) it is quite easy to obtain the effective V_3 potential. Since only measurements in the torsional ground state ($v = 0$) were used, it is not possible to discriminate between V_3, V_6 and higher order terms. The experimental and ab initio V_3 values show the same behavior as s does. The theoretical V_6 result has no experimental counterpart.

For comparison the V_3 values of *o*-chlorotoluene is given with those of similar molecules in Table 5. Obviously, $V_3 = 5.527(10)$ kJ mol^{-1} is an average value for this kind of molecule. Even, if the barriers are roughly confirmed by quantum chemical calculations, an intuitive interpretation turns out to be difficult. The most important influence of the substituent on the barrier seems to be of steric nature. A voluminous substituent like a chlorine atom or a methyl group leads to a high torsional barrier whereas a small or slim substituent like a fluorine atom or a cyano group hinders internal rotation much less.

5.3. Chlorine nuclear quadrupole coupling

The chlorine quadrupole coupling constants obtained from the least squares fits of the A and E species transitions, respectively, agree within their standard deviations (Table 2). All calculations carried out in this chapter are based on the data of the A species, but similar results can be obtained from the E state constants.

From molecular symmetry it is obvious that the principal axis of inertia c and of the chlorine quadrupole coupling tensor y coincide (see Fig. 2). Therefore,

$\chi_{yy} = \chi_{cc} = -\chi_{aa} - \chi_{bb}$ and the respective coupling constants $\chi_{cc}(^{35}\mathrm{Cl}) = 31.55845(169)$ MHz and $\chi_{cc}(^{37}\mathrm{Cl}) = 24.87423(222)$ MHz may be directly compared. The ratio $\chi_{cc}(^{35}\mathrm{Cl})/\chi_{cc}(^{37}\mathrm{Cl}) = 1.26872(13)$ is in excellent agreement with the value 1.26889(3) obtained from BrCl by Legon and Thorn [22].

Diagonalization of the coupling tensor, which has been obtained in inertial axes in the spectral analysis, is achieved by a rotation around the c axis. In the case of ^{35}Cl an angle $\angle(z, a) = 7.77(27)°$ is found, for ^{37}Cl $\angle(z, a) = 6.37(46)°$. These angles are in reasonable agreement with those between the C–Cl bond axis and the a axis obtained from ab initio calculations on MP2/6-311+G(2df,2p) level $(\angle(z, a)(^{35}\mathrm{Cl}) = 7.27°$, $\angle(z, a)(^{37}\mathrm{Cl}) = 6.48°)$. No indication for a bent bond was found. The coupling constant $\chi_{zz}(^{35}\mathrm{Cl}) = -69.953(144)$ MHz agrees well with those of chlorobenzene, *o*-chlorophenol, and *p*-chlorotoluene, whereas χ_{zz} of *o*-chlorofluorobenzene and *o*-dichlorobenzene is by 5% more negative (Table 6). The asymmetry of the coupling tensor $\eta = (\chi_{yy} - \chi_{xx})/\chi_{zz}$, which is a measure for the contribution of π orbitals, was found to be 0.0977. The η's of other chlorobenzene derivatives vary between 0.07 and 0.12. The number of p_y electrons lost as a result of double bonding can be calculated using Goldstein's [26] relation $\delta = (\chi_{xx} - \chi_{yy})/164.6$ MHz. For *o*-chlorotoluene we found $\delta = 0.0415$ (4.15%).

Comparing the coupling constants of *o*-chlorotoluene with those of other molecules in detail (Table 6) it fits into the series like a textbook example. Halogens are known as having a $+M$ (positive mesomeric) effect and therefore, injecting electrons into the ring system via a

Table 6
Quadrupole coupling constants of [^{35}Cl]-chlorobenzene derivatives

		χ_{zz} (MHz)	η	Ref.
o-Chlorophenol	*o*-(OH,Cl)–C$_6$H$_4$	−69.4758(84)	0.0045	[30]
o-Chlorotoluene	*o*-(CH$_3$,Cl)–C$_6$H$_4$	−69.953(144)	0.0977	This work
Chlorobenzene	Cl–C$_6$H$_5$	−71.241(7)	0.0734	[31]
p-Chlorotoluene	*p*-(CH$_3$,Cl)–C$_6$H$_4$	−71.7(7)		[7]
o-Chlorofluorobenzene	*o*-(Cl,F)–C$_6$H$_4$	−74.1173(41)	0.0882	[32]
o-Dichlorobenzene	*o*-(Cl,Cl)–C$_6$H$_4$	−74.34(52)	0.1183	[31]
Methyl chloride	CH$_3$Cl	−74.7514(11)	0.0000	[33]

Note. Asymmetry parameter $\eta = (\chi_{yy} - \chi_{xx})/(\chi_{zz})$, y is perpendicular to the ring plane, z points (roughly) along the C–Cl bond.

partial double bond and strongly extracting electrons via the σ bond ($-I$ or negative inductive effect). A methyl group is known as having a small $+I$ and almost no M effect. Therefore, the chlorine of o-chlorotoluene can extract electrons from the ring a little bit easier than in chlorobenzene and much easier than in o-halogenotoluene. This results in an absolute value of χ_{zz}, which is a little bit smaller than that of chlorobenzene and much smaller than that of o-dichlorobenzene and o-chlorofluorobenzene. On the other hand the OH group is known to have a $-I$ and a strong $+M$ effect and injects electrons into the ring. The ring electrons could therefore be extracted easier from the chlorine in o-chlorophenol than in o-chlorotoluene, which results in a larger absolute value of χ_{zz} in o-chlorotoluene than in o-chlorophenol. As an example of a non-aromatic system also the coupling constant of methyl chloride is given in Table 6.

Acknowledgments

References

[1] H.D. Rudolph, H. Seiler, Z. Naturforsch. A20 (1965) 1682–1686.

[2] H.D. Rudolph, H. Dreizler, A. Jaeschke, P. Wendling, Z. Naturforsch. A22 (1967) 940–944.

[3] J. Susskind, J. Chem. Phys. 53 (1970) 2492–2501.

[4] D. Schwoch, H.D. Rudolph, J. Mol. Spectrosc. 57 (1975) 47–74.

[5] H.D. Rudolph, A. Trinkaus, Z. Naturforsch. A23 (1968) 68–76.

[6] H.D. Rudolph, K. Walzer, I. Krutzik, J. Mol. Spectrosc. 47 (1973) 314–339.

[7] G. Herberich, Z. Naturforsch. A22 (1967) 761–764.

[8] P. Diehl, P.M. Henrichs, W. Niederberger, Mol. Phys. 20 (1971) 139–145.

[9] K.P.R. Nair, K. Epple, Chem. Phys. Lett. 166 (1990) 146–152.

[10] K.P.R. Nair, J. Mol. Struct. 477 (1999) 251–254.

[11] T. Schaefer, R. Sebastian, F.E. Hruska, Chem. Phys. Lett. 189 (1992) 252–254.

[12] E.C. Richard, R.A. Walker, J.C. Weisshaar, J. Chem. Phys. 104 (1996) 4451–4469.

[13] U. Andresen, H. Dreizler, J.U. Grabow, W. Stahl, Rev. Sci. Instrum. 61 (1990) 3694–3699.

[14] S. Kassi, D. Petitprez, G. Wlodarczak, J. Mol. Struct. 517–518 (2000) 375–386.

[15] H. Hartwig, H. Dreizler, Z. Naturforsch A51 (1996) 923–932.

[16] H.M. Pickett, J. Mol. Spectrosc. 148 (1991) 371–377.

[17] J.K.G. Watson, in: J.R. Durig (Ed.), Vibrational Spectra and Structure, 6, Marcel Dekker, New York, 1977.

[18] M.J. Frisch, G.W. Trucks, H.B. Schlegel, G.E. Scuseria, M.A. Robb, J.R. Cheeseman, V.G. Zakrzewski Jr., J.A. Montgomery, R.E. Stratmann, J.C. Burant, S. Dapprich, J.M. Millam, A.D. Daniels, K.N. Kudin, M.C. Strain, O. Farkas, J. Tomasi, V. Barone, M. Cossi, R. Cammi, B. Mennucci, C. Pomelli, C. Adamo, S. Clifford, J. Ochterski, G.A. Petersson, P.Y. Ayala, Q. Cui, K. Morokuma, D.K. Malick, A.D. Rabuck, K. Raghavachari, J.B. Foresman, J. Cioslowski, J.V. Ortiz, A.G. Baboul, B.B. Stefanov, G. Liu, A. Liashenko, P. Piskorz, I. Komaromi, R. Gomperts, R.L. Martin, D.J. Fox, T. Keith, M.A. Al-Laham, C.Y. Peng, A. Nanayakkara, C. Gonzalez, M. Challacombe, P.M.W. Gill, B. Johnson, W. Chen, M.W. Wong, J.L. Andres, C. Gonzalez, M. Head-Gordon, E.S. Replogle, J.A. Pople, Gaussian 98, Revision A.7, Gaussian, Pittsburgh, PA, 1998.

[19] V. Szalay, A.G. Császár, M.L. Senent, J. Chem. Phys. 117 (2002) 6489–6492.

[20] V. Kellö, A.J. Sadlej, Mol. Phys. 89 (1996) 127–137.

[21] P. Pyykkö, Mol. Phys. 99 (2001) 1617–1629.

[22] A.C. Legon, J.C. Thorn, Chem. Phys. Lett. 215 (1993) 554–560.

[23] W. Gordy, R.L. Cook, Microwave molecular spectra, in: A. Weissberger (Ed.), Techniques of Chemistry, Wiley, New York, 1984.

[24] J. Kraitchman, Am. J. Phys. 21 (1953) 17–24.

[25] B.P. van Eijck, J. Mol. Spectrosc. 91 (1982) 348–362.

[26] J.H. Goldstein, J. Chem. Phys. 24 (1956) 106–109.

[27] N. Hansen, H. Mäder, T. Bruhn. Mol. Phys. 97 (1999) 587–595.

[28] S. Maiti, A.I. Jaman, R.N. Nandi, J. Mol. Spectrosc. 177 (1996) 29–33.

[29] A. Welzel, A. Hellweg, I. Merke, W. Stahl, J. Mol. Spectrosc. 215 (2002) 58–65.

[30] M. Onda, N. Okada, Y. Fujita, T. Odaka, J. Mol. Spectrosc. 214 (2002) 129–131.

[31] I. Merke, C. Keussen, H. Dreizler, M. Onda, Z. Naturforsch. A45 (1990) 1273–1280.

[32] M. Onda, T. Odaka, H. Miyazaki, M. Mori, I. Yamaguchi, Y. Niide, J. Mol. Spectrosc. 176 (1996) 17–22.

[33] G. Wlodarczak, D. Boucher, R. Bocquet, J. Demaison, J. Mol. Spectrosc. 116 (1986) 251–255.